# JOC Article

Generation and Characterization of Highly Strained Dibenzotetrakisdehydro[12]- and Dibenzopentakisdehydro[14]annulenes

Ichiro Hisaki,[†] Takeshi Eda,[†] Motohiro Sonoda,[†] Hiroyuki Niino,[‡] Tadatake Sato,[‡] Tomonari Wakabayashi,[§] and Yoshito Tobe*,[†]

Division of Frontier Materials Science, Graduate School of Engineering Science, Osaka University, and CREST, Japan Science and Technology Agency (JST), Toyonaka, Osaka 560-8531, Japan, Photonics Research Institute, National Institute of Advanced Industrial Science and Technology (AIST), Tsukuba, Ibaraki 305-8565, Japan, and Department of Chemistry, School of Science and Engineering, Kinki University, Higashi-osaka, Osaka 577-8502, Japan

tobe@chem.es.osaka-u.ac.jp

Received December 3, 2004
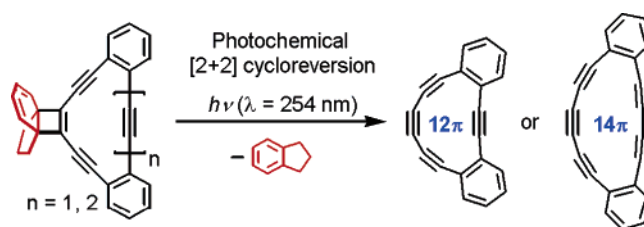
To generate dibenzotetrakisdehydro[12]- and dibenzopentakisdehydro[14]annulenes ([12]- and [14]-DBAs) having a highly deformed triyne moiety, [4.3.2]propellatriene-anneleted dehydro[12]- and dehydro[14]annulenes were prepared as their precursors. UV irradiation of the precursors resulted in the photochemical [2 + 2] cycloreversion to generate the strained [12]- and [14]DBAs, respectively. The [12]DBA was not detected by ^{1}H NMR spectroscopy, but it was intercepted as Diels−Alder adducts in solution, suggesting its intermediacy. Its spectroscopic characterization was successfully carried out by UV−vis spectroscopy in a 2-methyltetrahydrofuran (MTHF) glass matrix at 77 K and by FT-IR spectroscopy in an argon matrix at 20 K. On the other hand, the [14]DBA was stable enough for observation by ^{1}H and ^{13}C NMR spectra in solution, though it was not isolated because of the low efficiency of the cycloreversion. The [14]DBA was also characterized by interception as Diels−Alder adducts in solution and by UV−vis spectroscopy in a MTHF glass matrix at 77 K. The kinetic stabilities of the DBAs are compared with the related dehydrobenzoannulenes with respect to the topology of the π-systems. In addition, the tropicity of the [14]DBA is discussed based on its experimental and theoretical ^{1}H NMR chemical shifts.

Introduction

Dehydroannulenes and dehydrobenzoannulenes (DBAs) are the molecules that have been studied both experimentally and theoretically since the 1960s in connection with aromaticity−antiaromaticity of cyclic π-electron systems.[1] Recently, renewed interests on these molecules brought about the renaissance of the DBA chemistry,[2] in conjunction with the rapidly growing field of carbon-rich molecules,[3] in view of the following aspects. First, DBAs are potential materials for optoelectronic applications such as conducting and nonlinear optical (NLO) materials. For example, tribenzohexakisdehydro[18]-annulenes ([18]DBAs) with electron-donating and -accepting substituents are shown to possess considerable hyperpolarizabilities (β) for second-order NLO applica-

† Osaka University and Japan Science and Technology Agency (JST.
‡ National Institute of Advanced Industrial Science and Technology (AIST).
§ Kinki University.

(1) (a) Sondheimer, F. *Acc. Chem. Res.* **1972**, *5*, 81−91. (b) Sondheimer, F. *Chimia* **1974**, *28*, 163−172. (c) Nakagawa, M. *Pure Appl. Chem.* **1975**, *44*, 885−924.

(2) (a) Marsden, J. A.; Palmer, G. J.; Haley, M. M. *Eur. J. Org. Chem.* **2003**, 2355−2369. (b) Tobe, Y.; Sonoda, M. In *Modern Cyclophane Chemistry*; Gleiter, R., Hopf, H., Eds.; Wiley-VCH: Weinheim, Germany, 2004; pp 1−40.

(3) (a) Diederich, F.; Rubin, Y. *Angew. Chem., Int. Ed. Engl.* **1992**, *31*, 1101−1123. (b) Bunz, U. H. F.; Rubin, Y.; Tobe, Y. *Chem. Soc. Rev.* **1999**, *28*, 107−119. (c) de Meijere, A., Ed. Carbon Rich Compounds I. *Top. Curr. Chem.* **1998**, *196*. (d) de Meijere, A., Ed. Carbon Rich Compounds II. *Top. Curr. Chem.* **1999**, *201*.

tions.[4] Ladder oligomers of tribenzotrisdehydro[12]-annulene ([12]DBA) are predicted to exhibit increasing third-order NLO properties with increasing number of the [12]DBA units on the basis of the semiempirical molecular orbital calculations.[5] Second, certain members of DBAs are hypothetical constituent units of the hitherto unknown two-dimensional carbon networks[3,6] (e.g., graphyne or graphdiyne). In this respect, a number of topologically unique, highly extended π-systems consisting of [18]- and [12]DBAs has been reported.[2,7,8] Third, DBAs would serve as precursors of novel forms of all-carbon and carbon-rich materials. Thus, onion- and tube-like closed shell carbon clusters were formed by explosive decomposition of twisted [20]DBA[9] or organometallic derivatives of [18]- and [20]DBAs.[10] Moreover, a regular polymer was formed by topochemical polymerization of a [14]DBA containing strained triple bonds.[11] In addition to these materials-oriented interests, owing to the recent advances in theoretical as well as experimental assessment of tropicity, i.e., induced ring currents, many DBAs were prepared and their tropicity was examined. These include the theoretical study of Vollhardt,[12] Sundholm,[13] and Elguero[14] on various DBAs on the basis of nucleus-independent chemical shifts (NICS),[15] the theoretical and experimental studies on the DBAs fused by a cyclobutadiene or cyclopentadienide ring by Bunz[16] and on the [14]-DBAs fused by benzene rings[17] or a dimethyldihydropyrene ring,[18] the unit developed by Mitchell as a probe to estimate the aromaticity of fused rings,[19] by Haley and Williams.

From these points of view, we became interested in the title compounds, dibenzotetrakisdehydro[12]- and dibenzopentakisdehydro[14]annulenes ([12]- and [14]DBAs) **1a** and **1b** having a highly strained triyne component. These molecules are expected to give information regarding aromaticity of highly distorted π-systems. In particular, extremely strained [12]DBA **1a** possessing a remarkably deformed triyne unit would provide information about the stability and reactivity of the elusive all-carbon cyclic polyynes called cyclocarbons.[20-22] Additionally, such highly reactive species are also expected to transform into carbon clusters by (explosive) decomposition or extended propeller-shaped π-systems, tris(dehydrobenzo[12]annulene) **2a** and tris(dehydrobenzo[14]annulene) **2b**, by [2 + 2 + 2] cyclotrimerization, since such remarkable reactions have been known.[23]

1a　**1b**

2a　**2b**
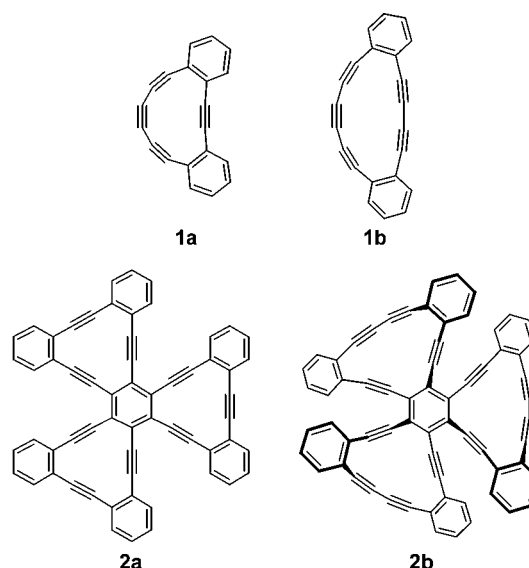
We planned to generate **1a** and **1b** from the respective precursors **3a** and **3b**, possessing a [4.3.2]propellatriene unit as a leaving group, by photochemical [2 + 2] cycloreversion of their cyclobutene rings extruding indan as shown in Scheme 1. We have already reported that various highly reactive polyynes were generated success-

(4) (a) Sarkar, A.; Pak, J. J.; Rayfield, G. W.; Haley, M. M. *J. Mater. Chem.* **2001**, *11*, 2943–2945.

(5) Zhou, Y.; Feng, S. *Solid State Commun.* **2002**, *122*, 307–310.

(6) Baughman, R. H.; Eckhardt, H.; Kertesz, M. *J. Chem. Phys.* **1987**, *87*, 6687–6699.

(7) For [18]DBA systems, see, for example: (a) Haley, M. M.; Brand, S. C.; Pak, J. J. *Angew. Chem.*, *Int. Ed. Engl.* **1997**, *36*, 836–838. (b) Wan, W. B.; Brand, S. C.; Pak, J. J.; Haley, M. M. *Chem. Eur. J.* **2000**, *6*, 2044–2052.

(8) For [12]DBA systems, see: (a) Kehoe, J. M.; Kiley, J. H.; English, J. J.; Johnson, C. A.; Petersen, R. C.; Haley, M. M. *Org. Lett.* **2000**, *2*, 969–972. (b) Miljanić, O. Š.; Vollhardt, K. P. C.; Whitener, G. D. *Synlett* **2002**, 29–34. (c) Iyoda, M.; Sirinintasak, S.; Nishiyama, Y.; Vorasingha, A.; Sultana, F.; Nakao, K.; Kuwatani, Y.; Matsuyama, H.; Yoshida, M.; Miyake, Y. *Synthesis* **2004**, 1527–1531. (d) Sonoda, M.; Sakai, Y.; Yoshimura, T.; Tobe, Y.; Kamada, K. *Chem. Lett.* **2004**, *33*, 972–973.

(9) Boese, R.; Matzger, A. J.; Vollhardt, K. P. C. *J. Am. Chem. Soc.* **1997**, *119*, 2052–2053.

(10) (a) Dosa, P. I.; Erben, C.; Iyer, V. S.; Vollhardt, K. P. C.; Wasser, I. M. *J. Am. Chem. Soc.* **1999**, *121*, 10430–10431. (b) Laskoski, M.; Steffen, W.; Morton, J. G. M.; Smith, M. D.; Bunz, U. H. F. *J. Am. Chem. Soc.* **2002**, *124*, 13814–13818.

(11) Baldwin, K. P.; Matzger, A. J.; Scheiman, D. A.; Tessier, C. A.; Vollhardt, K. P. C.; Youngs, W. J. *Synlett* **1995**, 1215–1218.

(12) Matzger, A. J.; Vollhardt, K. P. C. *Tetrahedron Lett.* **1998**, *39*, 6791–6794.

(13) Jusélius, J.; Sundholm, D. *Phys. Chem. Chem. Phys.* **2001**, *3*, 2433–2437.

(14) Alkorta, I.; Rozas, I.; Elguero, J. *Tetrahedron* **2001**, *57*, 6043–6049.

(15) Schleyer, P. v. R.; Maerker, C.; Dransfeld, A.; Jiao, H.; Hommes, N. J. R. v. E. *J. Am. Chem. Soc.* **1996**, *118*, 6317–6318.

(16) (a) Laskoski, M.; Steffen, W.; Smith, M. D.; Bunz, U. H. F. *Chem. Commun.* **2001**, 691–692. (b) Laskoski, M.; Smith, M. D.; Morton, J. G. M.; Bunz, U. H. F. *J. Org. Chem.* **2001**, *66*, 5174–5181. (c) Boydston, A. J.; Laskoski, M.; Bunz, U. H. F.; Haley, M. M. *Synlett* **2002**, 981–983.

(17) (a) Boydston, A. J.; Haley, M. M. *Org. Lett.* **2001**, *3*, 3599–3601. (b) Boydston, A. J.; Haley, M. M.; Williams, R. V.; Armantrout, J. R. *J. Org. Chem.* **2002**, *67*, 8812–8819.

(18) Kimball, D. B.; Haley, M. M.; Mitchell, R. H.; Ward, T. R.; Bandyopadhyay, S.; Williams, R. V.; Armantrout, J. R. *J. Org. Chem.* **2002**, *67*, 8798–8811.

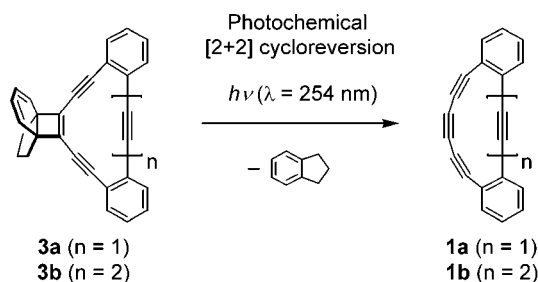(19) Mitchell, R. H. *Chem. Rev.* **2001**, *101*, 1301–1315.

(20) (a) Diederich, F. In *Modern Acetylene Chemistry*; Stang, P. J., Diederich, F., Eds.; VCH: Weinheim, 1995; pp 443–471. (b) Diederich, F.; Gobbi, L. *Top. Curr. Chem.* **1999**, *201*, 43–79. (c) Diederich, F.; Rubin, Y.; Knobler, C. B.; Whetten, R. L.; Schriver, K. E.; Houk, K.; Li, Y. *Science* **1989**, *245*, 1088–1090. (d) Rubin, Y.; Kahr, M.; Knobler, C. B.; Diederich, F.; Wilkins, C. L. *J. Am. Chem. Soc.* **1991**, *113*, 495–500. (e) McElvany, S. W.; Ross, M. M.; Goroff, N. S.; Diederich, F. *Science* **1993**, *259*, 1594–1596. (f) Diederich, F.; Rubin, Y.; Chapman, O. L.; Goroff, N. S. *Helv. Chim. Acta* **1994**, 77, 1441–1457.

(21) (a) Tobe, Y. In *Advances in Strained and Interesting Organic Molecules*; Halton, B., Ed.; JAI Press: Stamford, 1999; Vol. 7, pp 153–184. (b) Tobe, Y.; Fujii, T.; Matsumoto, H.; Naemura, K.; Achiba, Y.; Wakabayashi, T. *J. Am. Chem. Soc.* **1996**, *118*, 2758–2759. (c) Tobe, Y.; Matsumoto, H.; Naemura, K.; Achiba, Y.; Wakabayashi, T. *Angew. Chem., Int. Ed. Engl.* **1996**, *35*, 1800–1802. (d) Wakabayashi, T.; Kohno, M.; Achiba, Y.; Shiromaru, H.; Momose, T.; Shida, T.; Naemura, K.; Tobe, Y. *J. Chem. Phys.* **1997**, *107*, 4783–4787. (e) Tobe, Y.; Fujii, T.; Matsumoto, H.; Tsumuraya, K.; Noguchi, D.; Nakagawa, N.; Sonoda, M.; Naemura, K.; Achiba, Y.; Wakabayashi, T. *J. Am. Chem. Soc.* **2000**, *122*, 1762–1775.

(22) Tobe, Y.; Umeda, R.; Iwasa, N.; Sonoda, M. *Chem. Eur. J.* **2003**, *9*, 5549–5559.

(23) For cyclotrimerization of highly deformed alkynes, see, for example: (a) Chapman, O. L.; Gano, J.; West, P. R.; Regitz, M.; Maas, G. *J. Am. Chem. Soc.* **1981**, *103*, 7033–7036. (b) Iglesias, B.; Peña, D.; Pérez, D.; Guitián, E.; Castedo, L. *Synlett* **2002**, 486–488.
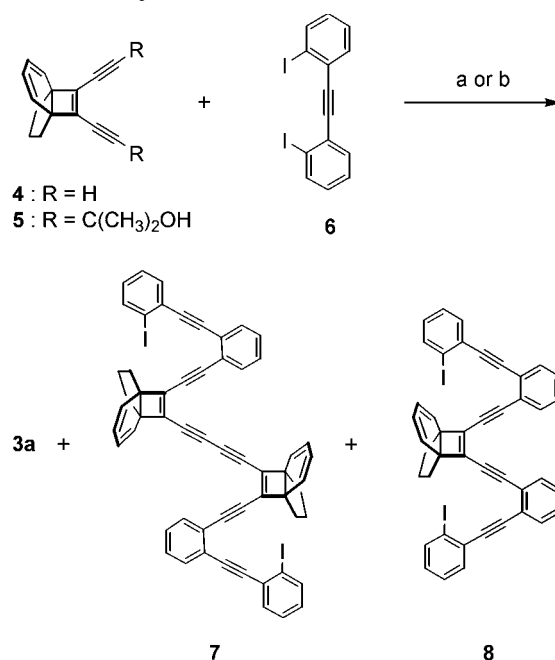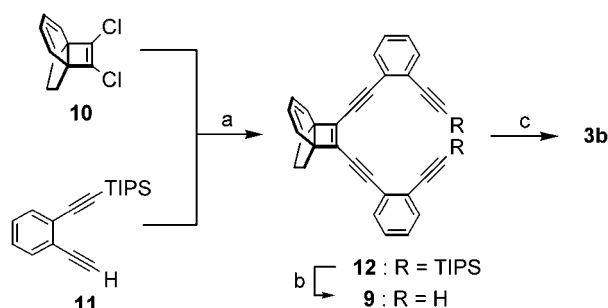
SCHEME 1

SCHEME 2. Synthesis of Precursor 3a[a]

[a] Reaction conditions: (a) Pd(PPh₃)₄, CuI, Et₃N, 60 °C, **3a**, 1%; (b) Pd(PPh₃)₄, CuI, PPh₃, CH₃N[(CH₂)₇CH₃]₃Cl, NaOH, H₂O, benzene, 80 °C, **3a**, 49%.

SCHEME 3. Synthesis of Precursor 3b[a]

[a] Reaction conditions: (a) Pd₂(dba)₃·CHCl₃, CuI, piperidine/THF (5:1 v/v), 60 °C, 41%; (b) TBAF, AcOH, THF, rt; (c) Cu(OAc)₂, pyridine, rt, 76% for the two steps.

fully from the corresponding precursors possessing the [4.3.2]propellatriene units by laser desorption in the gas phase as well as by photoirradiation in solution.[21,24] In this paper, we report the syntheses of propellatriene-annelated DBAs, **3a** and **3b**, generation of **1a** and **1b** by the photochemical [2 + 2] cycloreversion of the respective precursors **3a** and **3b**, and characterization of **1a** and **1b**.[25] Characterization in solution was carried out by the ¹H and ¹³C NMR spectra (only for **1b**) and by their interception as Diels−Alder adducts. Spectroscopic identification of **1a** and **1b** was done by the measurements of the UV−vis spectra in a 2-methyltetrahydrofuran (MTHF) glass matrix at 77 K and FT-IR (only for **1a**) in an argon matrix at 20 K in conjunction with their theoretical predictions. The kinetic stability of **1a** and **1b** is compared with that of the related DBAs with respect to the topology of the π-systems. In addition, the tropicity of [14]DBA **1b** is discussed based on its experimental and theoretical ¹H NMR chemical shifts.

Results and Discussion

Syntheses of Propellane-Annelated [12]- and [14]-DBAs 3a and 3b. Propellane-anneleted [12]DBA **3a** was prepared by Pd-catalyzed 1:1 cross-coupling of diethynylpropellatriene **4**[21c,e] or its derivative **5**[21c,e] with bis-(2-iodophenyl)acetylene (**6**)[26] (Scheme 2). First, reaction of **4** with **6** was attempted. To our dismay, the reaction typically gave a complex mixture of products containing **3a** in as low as 1% yield. As byproducts, 2:2 coupling product **7** (2%) and 1:2 coupling product **8** (6%) were characterized, but most of the products were uncharacterized polymeric materials. Gratifyingly, however, by in situ deprotection and intermolecular cross-coupling reaction[27] of **5** and **6** under the phase-transfer conditions, 49% yield of **3a** was achieved. Synthesis of the precursor **3b** was accomplished by intramolecular oxidative coupling of **9** as shown in Scheme 3. Thus, dichloropropellatriene **10**[21c,e] was cross-coupled to 2-ethynyl-1-(triisopropylsilyl)-

ethynylbenzene (**11**)[28] to give acyclic tetrayne **12** in 41% yield. Desilylation of **12** followed by Cu(II)-mediated oxidative coupling under high dilution conditions gave **3b** in 76% yield.

UV−vis spectra of the precursors **3a** and **3b** are shown in Figure 1. Both spectra exhibit similar profile in the wavelength region shorter than 400 nm, with the spectrum of **3b** being red-shifted by 20 nm compared to that of **3a**. However, the end absorption of **3a** extends considerably to the longer wavelength than that of **3b**, reflecting the antiaromatic character of **3a**.

Geometries of Precursors and Highly Strained Dehydroannulenes. To investigate the geometries of the precursors **3a** and **3b** and respective strained DBAs **1a** and **1b**, their optimized geometries were calculated by the DFT method at the B3LYP/6-31G* level as shown

(24) (a) Tobe, Y.; Nakagawa, N.; Naemura, K.; Wakabayashi, T.; Shida, T.; Achiba, Y. *J. Am. Chem. Soc.* **1998**, *120*, 4544−4545. (b) Tobe, Y.; Nakanishi, H.; Sonoda, M.; Wakabayashi, T.; Achiba, Y. *Chem. Commun.* **1999**, 1625−1626. (c) Tobe, Y.; Nakagawa, N.; Kishi, J.; Sonoda, M.; Naemura, K.; Wakabayashi, T.; Shida, T.; Achiba, Y. *Tetrahedron* **2001**, *57*, 3629−3636. (d) Tobe, Y.; Furukawa, R.; Sonoda, M.; Wakabayashi, T. *Angew. Chem., Int. Ed.* **2001**, *40*, 4072−4074.

(25) For preliminary reports of this work, see: (a) Tobe, Y.; Ohki, I.; Sonoda, M.; Niino, H.; Sato, T.; Wakabayashi, T. *J. Am. Chem. Soc.* **2003**, *125*, 5614−5615. (b) Hisaki, I.; Eda, T.; Sonoda, M.; Tobe, Y. *Chem. Lett.* **2004**, *33*, 620−621.

(26) Kowalik, J.; Tolbert, L. M. *J. Org. Chem.* **2001**, *66*, 3229−3231.

(27) (a) Huynh, C.; Linstrumelle, G. *Tetrahedron* **1988**, *44*, 6337−6344. For the use of tricaprylmethylammonium salt in this reaction, see: (b) Ohkita, M.; Ando, K.; Suzuki, T.; Tsuji, T. *J. Org. Chem.* **2000**, *65*, 4385−4390.

(28) Bell, M. L.; Chiechi, R. C.; Johnson, C. A.; Kimball, D. B.; Matzger, A. J.; Wan, W. B.; Weakley, T. J. R.; Haley, M. M. *Tetrahedron* **2001**, *57*, 3507−3520.
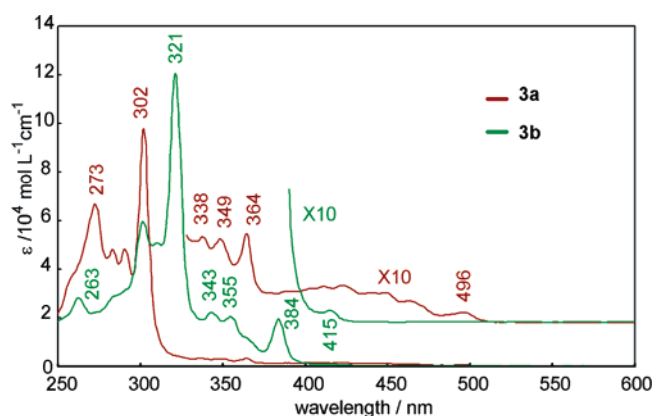
FIGURE 1. UV−vis spectra of precursor **3a** (red) and **3b** (green) in CHCl$_3$ at 303 K. Expanded spectra are shifted vertically for clarity.

in Figure 2. The triple bonds of **3a** attached the cyclobutene ring are slightly distorted to outward, while the corresponding bonds of **3b** are nearly straight. In contrast to the small bond angle distortion in the annulene rings of the precursors **3a** and **3b**, DBAs **1a** and **1b** exhibit noticeable distortions particularly in their triyne moieties as shown in Figure 2a,b. While the energy-minimum structures of **1a** and **1b** are not symmetrical with respect to the plane bisecting the triyne unit, the

transition state between the two unsymmetrical geometries possesses C$_{2v}$ symmetrical geometry. However, the energy differences between the ground and transition states are small; ca. 2.2 cal/mol for **1a** and ca. 38 cal/mol for **1b**. The most remarkable geometrical characteristic of **1a** is the fact that the C≡C−C bonds in the triyne component of **1a** are highly deformed from linearity by 32.9−15.0° for the ground state and by 31.0−15.9° for the transition state. In the ground state, bond angle of the most strained central triyne unit is predicted to be as small as 147.1°! By contrast, the C$_2$ bridge of **1a** is predicted to be slightly deformed to the inside of the annulene ring by 7.2−7.6°, making both the C$_2$ and C$_6$ bridges curve to the same direction. On the other hand, the triyne unit of **1b** is not as strained as that of **1a**, but it is still considerably deformed; the bending angles are 22.4−15.6° for the ground state and 19.0−12.8° for the transition state. The diyne unit of **1b** is much less distorted with the bending angles of 3.5−5.2° (ground state) and 3.9−4.3° (transition state). With regard to the bond lengths, there is larger bond length alternation in the 12-membered rings of [12]DBAs **1a** and **3a** in comparison with that of the 14-membered rings of the respective [14]DBAs **1b** and **3b**, owing to their nonaromatic and aromatic characters, respectively. On the contrary, the bond alternation of the benzene rings of **1a** and **3a** are smaller than those of the respective [14]-
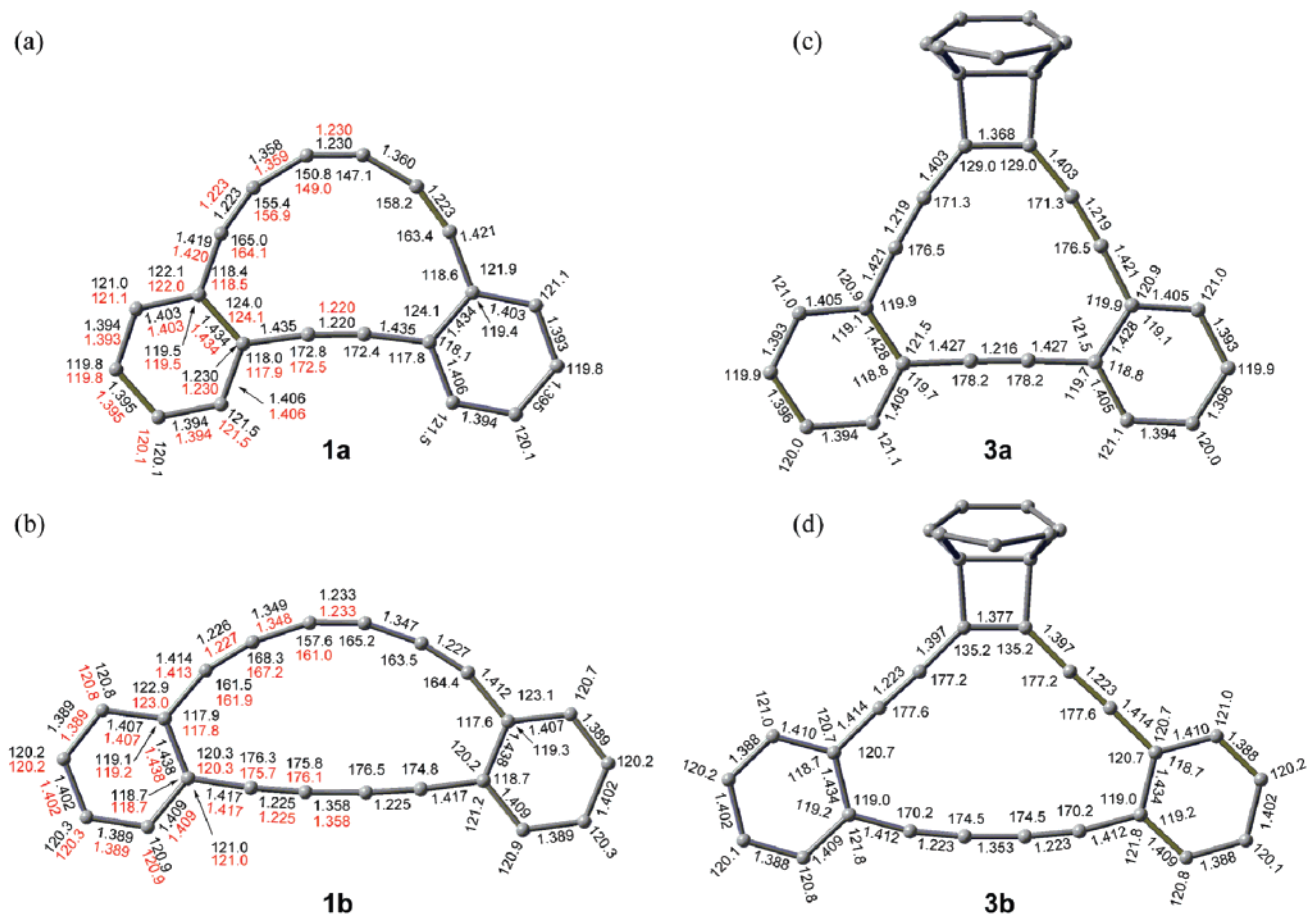
FIGURE 2. Optimized geometries of (a) **1a**, (b) **1b**, (c) **3a**, and (d) **3b** calculated by the DFT method at the B3LYP/6-31G* level. Selected bond lengths (Å) and angles (deg) are shown in black for the ground-state structures and in red for the transition-state structures having C$_{2v}$ symmetry. Hydrogen atoms are omitted for clarity.

annulenes **1b** and **3b** for the same reason. However, the bond lengths of the benzene rings within the [12]DBA derivatives **1a** and **3a** or within the [14]DBA derivatives **1b** and **3b** are similar to each other, suggesting that the tropicity of the annulene rings within each series is not much different.

To examine the bond length alternation of **3a** and **3b** experimentally, their X-ray structural analysis was undertaken. Recrystallization of **3a** and **3b** from CH_2-Cl_2/hexane afforded single crystals with sufficient quality for X-ray structural analysis. The structures are shown in Figures S17 and S18, respectively, in the Supporting Information. Both the 12- and 14-membered rings of **3a** and **3b** are planer. Angles of the $C≡C-C$ bond in **3a** determined by X-ray structural analysis were slightly smaller than those predicted by the DFT calculations (ca. 2.3−0.3°), while in the case of **3b**, no constant tendency was observed in this respect. With regard to the bond lengths, the calculated structures seem to underestimate the bond length alternation of the annulene rings of **3a** and **3b** compared with the respective X-ray structures; for example, the bond lengths of C1−C2, C2≡C3, and C3−C4 of **3b** are 1.397, 1.219, and 1.424 Å, respectively, in the theoretical geometries, while those are 1.411, 1.199, and 1.427 Å in the observed structures, respectively. As observed in the theoretical structures **3a** and **3b**, larger bond length alternation in the 12-membered ring of **3a** was observed in comparison with that of the 14-membered ring of **3b** in the X-ray structures, although the degree of alternation is smaller than that in the calculated geometries.

Photolysis of 3a and 3b in Solution. As a preliminary study of the photochemical [2 + 2] cycloreversion, a solution of **3a** in THF-d_8 (2.1×10^{-2} M) was irradiated at room temperature with a low-pressure mercury lamp and the reaction was monitored by ^{1}H NMR spectra. Upon irradiation, the signals of **3a** decreased, and instead, the signals ascribed to indan appeared, indicating that [2 + 2] cycloreversion of **3a** took place. However, any signal ascribable to **1a** was not observed. On the other hand, the signals at 6.35−6.29 and 3.27−3.24 ppm appeared, which we assigned to the vinyl and the methine protons on the bridgeheads, respectively, of **13a** derived by [4 + 2] addition between **1a** and **3a** as shown in Scheme 4 (see Figure S1 in Supporting Information for the NMR spectrum.). We also observed a peak in the LC−MS analysis of the photolysate at *m/z* 615.4 corresponding to [**13a** + 1]$^+$. By preparative scale photolysis of **3a** in THF, [4 + 2] adduct **13a** was isolated in 18% yield as a yellow solid. In addition, irradiation of **3a** in furan gave the furan adduct **14a** in 20% yield as an orange solid. X-ray crystallographic structures of **13a** and **14a** shown in Figures S19 and S20, respectively, in the Supporting Information revealed that the propellane unit of **3a** was replaced by another molecule of **3a** and furan, respectively, indicating that the addition took place at the central, most strained triple bond of the triyne unit of **1a**. These results indicate that the photolysis of **3a** leads to the generation of **1a**, but it is too reactive for characterization by spectroscopic methods in solution.

As shown in Figure S19 in the Supporting Information, the adduct **13a** possesses two [12]DBA units pointing to the opposite directions. This indicates that the reactive intermediate **1a** added to the cyclohexadiene moiety of

SCHEME 4

syn adduct **13a**   *anti* adduct
   not observed
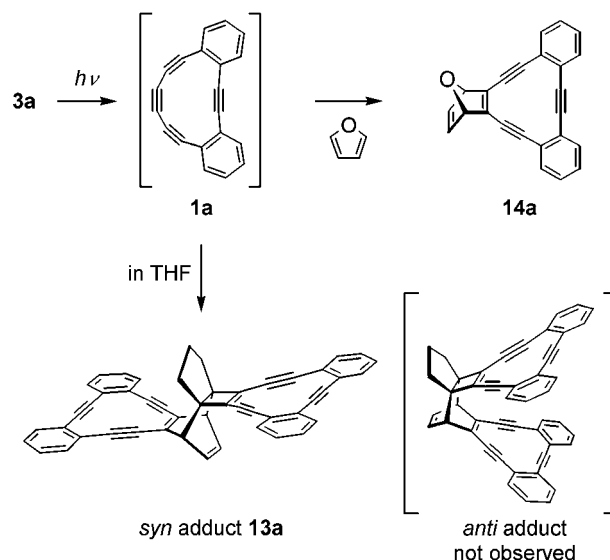
3a from the same side of the cyclopentane ring. This selectivity can be explained in terms of steric effect of the propellane moiety of **3a**.[29] Namely, the dihedral angle between the cyclohexadiene and cyclopentane rings (131°) is wider than that between the cyclohexadiene and cyclobutene rings (116°) as revealed by the X-ray analysis.[30]

On the other hand, we were able to observe the ^{1}H and ^{13}C NMR signals due to **1b** which was generated by photolysis of the precursor **3b** with a low-pressure mercury lamp in a THF-d_8 solution at 213−220 K. The ^{1}H NMR spectrum of **3b** in THF-d_8 (1.1×10^{-2} M) and its change upon irradiation for 24 h at 220 K are shown in Figure 3. Irradiation of **3b** brought about the appearance of two new multiplets at 7.93−7.91 and 7.63−7.57 ppm, with a relative integration of 1:3, in addition to those of indan as shown in Figure 3b. These new signals are in good agreement with the theoretical chemical shifts of the aromatic protons in **1b** calculated by the GIAO-B3LYP/6-31G*//B3LYP/6-31G* calculations as described later. The conversion of **3b** to **1b**, however, remained low (ca. 19%) even after prolonged irradiation because of the absorption of the incident light by the photoproducts **1b** and indan. Irradiation of a more dilute solution of **3b** (1.3×10^{-3} M) in THF-d_8 for 6 h at 213 K resulted in better conversion (ca. 31%) (Figure 3, inset). However, further irradiation of this solution did not push the reaction to completion. Rather, the intensity of the signals of **1b** decreased presumably because of undesirable decomposition of **1b**. By standing the solution of (b) for 65 h at 303 K, the signals assigned to **1b** disappeared and two signals at 6.47−6.45 and 4.29−4.27 ppm appeared albeit in low intensities. These signals are ascribed to the vinyl protons (H_g) and the bridgehead protons (H_h) of the [4 + 2] adduct **13b**, in view of the chemical shifts of the corresponding protons of **13a** mentioned above. This [4 + 2] adduct **13b** was also detected by LC-MS analysis
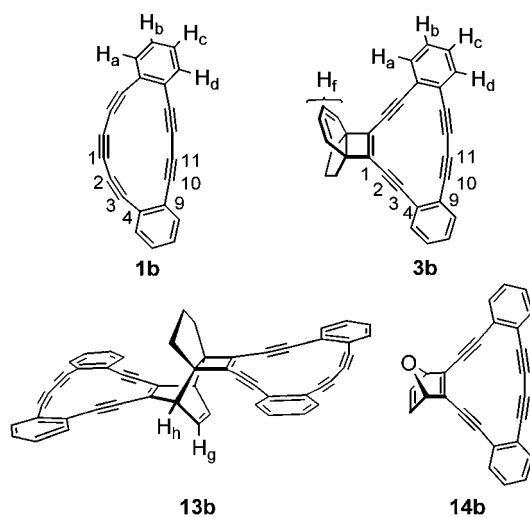
(29) Tsuji, T.; Ohkita, M.; Nishida, S. *J. Org. Chem.* **1991**, *56*, 997−1003.

(30) The cyclohexadiene, cyclopentane, and cyclobutene rings of the [4.3.2]propellatriene unit of **3a** are defined by the least-squares planes consist of the bridgehead carbon atoms and their adjacent carbon atoms.
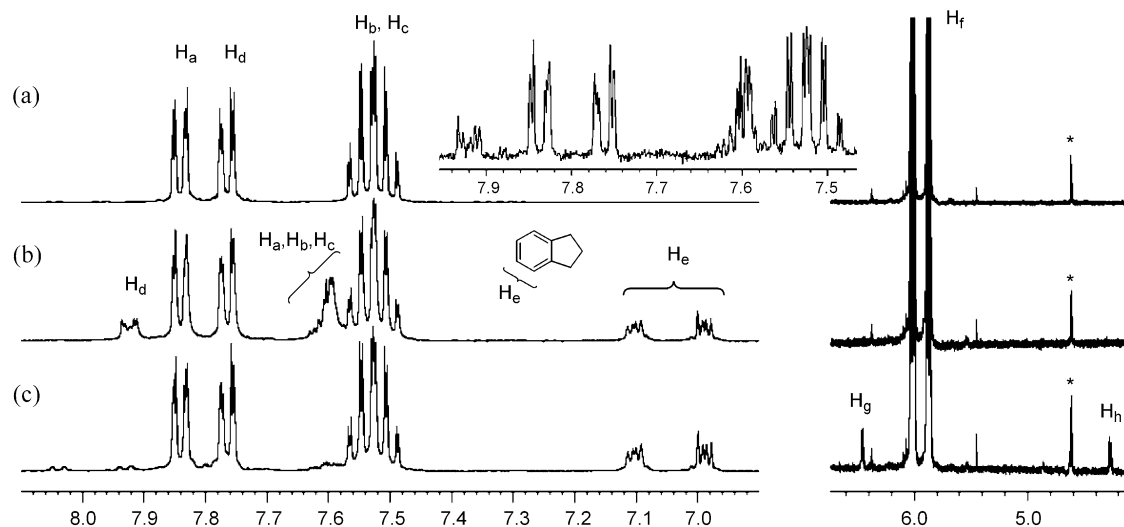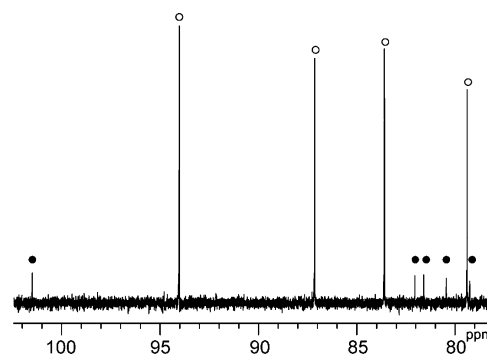
FIGURE 3. ^{1}H NMR spectral change of **3b** upon photolysis in THF-d_8 (1.1×10^{-2} M) (a) before irradiation, (b) after irradiation for 24 h at 220 K, (c) after standing the solution of (b) for 65 h at 303 K. (Inset) spectrum of a more dilute solution of **3b** (1.3×10^{-3} M) after irradiation for 6 h at 210 K.

(m/z 663.5) of the solution, though we were unable to isolate it because of the low efficiency of its formation. The [4 + 2] adduct **14b** of **3b** with furan was isolated by irradiation of **3b** in furan. However, unlike the case of **3a**, a large amount of polymeric materials were formed and isolated yield of **14b** was very low (ca. 2%). In the ^{1}H NMR spectrum of **14b**, the vinyl protons and the bridgehead protons resonate at 7.30 and 5.88 ppm, respectively, which are downfield shifted relative to those of **14a** by 0.26 and 0.60 ppm, respectively. These downfield shifts are attributed to the diamagnetic ring current of the [14]annulene ring of **14b**. The lower yields of [4 + 2] adduct **13b** and **14b** than those of **13a** and **14a** indicate that the central triple bond of the triyne moiety of **1b** is much less reactive toward thermal cycloaddition than that of **1a**.

FIGURE 4. Partial ^{13}C NMR spectrum of **3b** after irradiation in THF-d_8 for 24 h at 213 K. Marked resonances are due to **3b** (○) and **1b** (●), respectively.

with the signals of **3b**, one signal appears at distinctly low field, while the other four signals seem to move upfield. To assign the remarkably downfield shifted carbon signal of **1b**, theoretical chemical shifts were estimated by the GIAO-B3LYP/6-31G* calculations. As a result, C1, C2, C3, C10, and C11 are predicted to resonate at 78.8, 79.9, 101.2, 80.0, and 79.1 ppm, respectively, indicating that the signal in question should be assigned to C3. It was reported that the sp carbon atoms of diphenylhexatriyne (**15a**) resonate at 66.4, 74.4, and 78.6 ppm[31] and those of [20]DBA **16** having a slightly strained triyne unit resonate at 68.9–81.6 ppm,[32] suggesting that the distinctly deshielded resonance observed for **1b** is due to the considerable distortion of its triyne unit. To estimate the effect of distortion on the ^{13}C NMR chemical shifts of diphenylhexatriyne (**15a**), the chemical shifts of **15a** and hypothetical triyne **15b** having the same bending angles as those of the triyne unit of **1b** were estimated by the same theoretical method. The calculated chemical shifts (**15a**: C1 64.3, C2 73.7, C3 72.2 ppm, **15b**: C1 77.0, C2 74.2, C3 101.3 ppm) clearly indicate

The ^{13}C NMR spectrum obtained after irradiation of a solution of **3b** in THF-d_8 (3.4×10^{-2} M) for 24 h at 213 K is shown in Figure 4. Besides the signals of the sp carbons of unphotolyzed **3b** at 94.0, 87.1, 83.6, and 79.4 ppm, five weak signals at 101.4, 82.6, 81.6, 80.4, and 79.2 ppm are observed, which we ascribe to **1b**. Compared
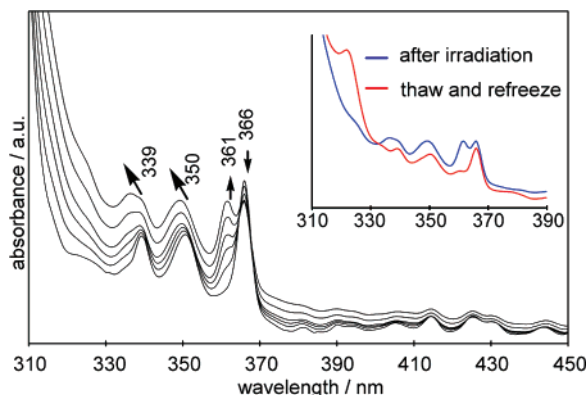
(31) Orita, A.; Yoshioka, N.; Struwe, P.; Braier, A.; Beckmann, A.; Otera, J. *Chem. Eur. J.* **1999**, *5*, 1355–1363.
(32) Wan, W. B.; Kimball, D. B.; Haley, M. M. *Tetrahedron Lett.* **1998**, *39*, 6795–6798.
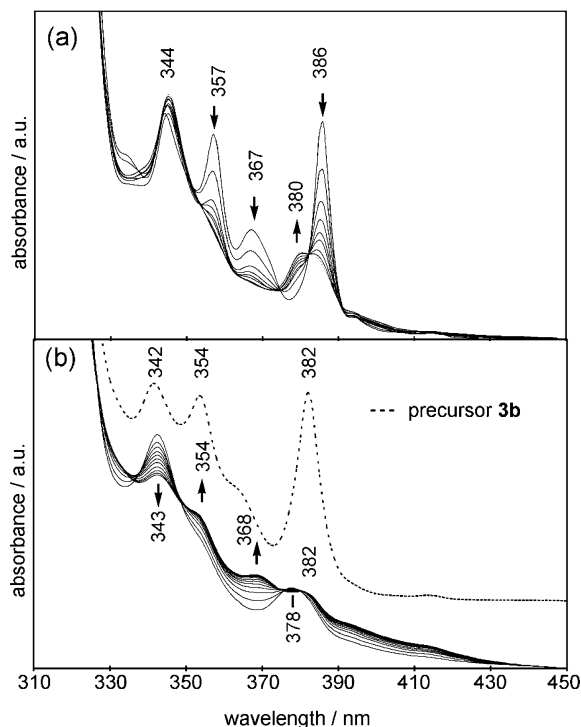
FIGURE 5. UV–vis spectral change of **3a** upon irradiation for 14 h in MTHF matrix at 77 K. (Inset) comparison between spectrum after irradiation (blue line) and that after thaw and refreeze (red line).

that C3 experiences the most remarkable downfield shift owing to the bending of the triple bonds. This is probably attributed to the large decrease of charge at C3 by bending the triple bonds.[33] Thus, although [14]DBA **1b** was stable enough for characterization by ^{1}H and ^{13}C NMR spectroscopy in solution, we were unable to isolate it because of its high reactivity and the low efficiency of its generation.
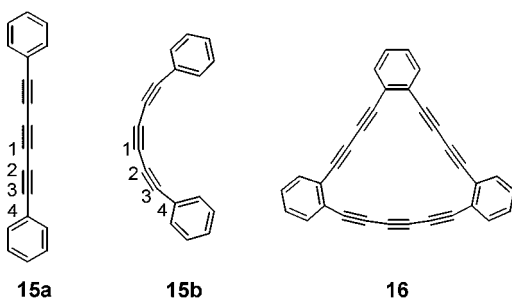
Photolysis of 3a and 3b in 2-Methyltetrahydrofuran (MTHF) Matrices. In order for UV–vis spectroscopic characterization of **1a** and **1b**, precursors **3a** and **3b** were dispersed in MTHF glass matrices at 77 K and irradiated with a low-pressure mercury lamp. In the case of **3a**, as shown in Figure 5, a new prominent absorption band due to a photoproduct at 361 nm grew simultaneously with the decay of that of **3a** at 366 nm.[34] Additionally, the bands of **3a** at 350 and 339 nm slightly shifted to shorter wavelength region. When the matrix was thawed by warming to room temperature and then refrozen at 77 K, the new absorption band at 361 nm was completely lost while the bands at 366, 350, and 339 nm due to unphotolized **3a** were still alive (Figure 5, inset), indicating the formation of a reactive intermediate, which we ascribed to **1a**. Similarly, by irradiation of **3b**, the intensity of the absorption bands of **3b** at 386, 367, and

FIGURE 6. (a) UV–vis spectral change of **3b** upon photolysis for 12 h in MTHF matrix at 77 K. (b) Spectral change of photolysate upon standing the thawed solution for 50 h at 303 K. For sake of comparison, the spectrum of precursor **3b** measured in a MTHF solution was shown by a dotted line, which is sifted vertically for clarity.

357 nm decreased dramatically, and a new band at 380 nm, which we ascribed to **1b**, grew simultaneously as shown in Figure 6a. In addition, the band of **3b** at 344 nm bathochromically shifted by 1 nm and its intensity increased slightly. After irradiation, the MTHF glass matrix was thawed by warming to 303 K, and the solution of the photolysate was kept at 303 K for 50 h. As shown in Figure 6b, upon standing the solution, the absorption bands due to **1b** at 343 and 378 nm became ambiguous owing to the gradual rise of the baseline. The weak bands increased at 368, 354, and 382 nm are ascribed to unphotolyzed **3b**, which presumably became apparent because of the rise of the baseline.

Characterization of 1a by FT-IR Spectroscopy. To characterize highly reactive **1a**, irradiation of the precursor **3a** was carried out in an argon matrix film at 20 K and the FT-IR spectra were measured. [12]DBA **1a** was identified by comparing the IR spectra observed experimentally with those theoretically calculated by the DFT method at the B3LYP/6-31G* level. It has been established that theoretical IR spectra predicted by the DFT calculation at this level can well reproduce the experimental spectra and, thus, can be used to identify the unusual molecules isolated in low-temperature matrices.[35]

The FT-IR spectrum in an argon matrix observed after irradiation are shown in Figure 7a. The observed spectrum of the precursor **3a** and indan are also shown as

(33) The calculations predict that the charges on C1, C2, and C3 atoms changed by −0.30, −0.40, and +0.72, respectively, upon bending of **15a** into **15b**.

(34) UV–vis spectroscopic measurement of **3a** was also carried out in an Ar matrix at 20 K to give an identical spectral change as that observed upon irradiation in MTHF matrix at 77 K.; decay of the band at 359 nm ascribed to **3a** and growth of the band at 355 nm due to formation of the new chemical species, presumably **1a** (see Figure S5 in the Supporting Information).

(35) (a) Scott, A. P.; Radom, L. *J. Phys. Chem.* **1996**, *100*, 16502–16513. (b) Sato, T.; Arulmozhiraja, S.; Niino, H.; Sasaki, S.; Matsuura, T.; Yabe, A. *J. Am. Chem. Soc.* **2002**, *124*, 4512–4521.
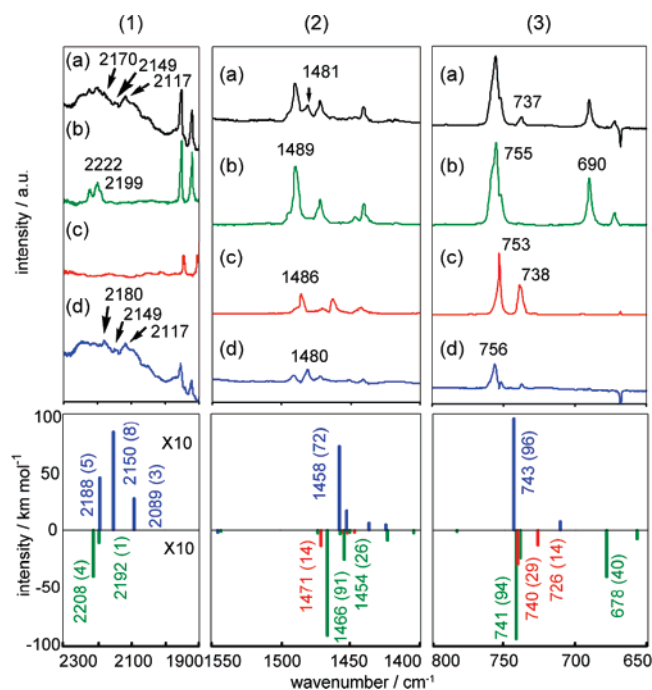
FIGURE 7. Selected FT-IR spectra of C−C stretching of acetylenes (column 1), in-plane C−H bending (column 2), and out-of-plane C−H bending (column 3) vibrations. (Top) observed spectra in an argon matrix at 20 K: (a) after irradiation, (b) precursor **3a**, (c) indan, and (d) differential spectra obtained by subtraction of (b) and (c) from (a); (Bottom) theoretical IR spectra calculated at the B3LYP/6-31G* level: precursor **3a** (green), **1a** (blue), and indan (red). Oscillation intensities are shown in parentheses.

spectra (b) and (c) in Figure 7. The spectrum (d) is the differential spectrum obtained by subtracting spectra (b) and (c) from (a) with appropriate scaling factors to remove the contribution from the latter two. Columns 1, 2, and 3 in Figure 7 show vibrational regions for C≡C stretching, C−H out-of-plane bending, and C−H in-plane bending modes, respectively, which are characteristic to **1a**, **3a**, and indan. In the observed spectrum after irradiation, two recognizable absorption bands at 1481 and 737 cm^{-1} appeared as shown in Figures 7(2)(a) and (3)(a), respectively, which can be attributed to indan by comparing with Figures 7(2)(c) and (3)(c). In the high-frequency region (spectrum (1)(a)), three weak IR bands at 2117, 2149, and 2170 cm^{-1} appeared, which may be ascribed to the C≡C stretching bands of **1a**, in addition to those of the precursor **3a** (2199 and 2222 cm^{-1}) which are shown in spectrum (1)(b).

In the bottom of Figure 7, the theoretical IR spectra of **1a**, **3a**, and indan are shown as blue, green, and red bars, respectively. The theoretical spectra of both **3a** and indan nicely reproduce those observed in the matrices, though the former spectra exhibit constant shift from the latter. For example, the predicted absorptions at 741 and 678 cm^{-1} for **3a** correspond to those observed at 755 and 690 cm^{-1}, respectively, and the theoretical bands at 740 and 726 cm^{-1} for indan are observed at 753 and 738 cm^{-1}, respectively. A similar tendency is observed in columns (1) and (2). Theoretical absorptions of **1a** are predicted to appear at 1458 cm^{-1} for C−H in-plane bending, 743 cm^{-1} for C−H out-of-plane bending, and 2188, 2150, and 2089 cm^{-1} for C≡C stretching. As shown in spectrum (d),

the corresponding bands are apparently observed in the differential spectrum at 1480, 756, and 2180, 2149, and 2117 cm^{-1}, respectively, though the intensities of the last three bands are very weak. Thus, the observed bands in spectrum (d) are, in total, in good agreement with the theoretical IR spectrum of **1a**. These results indicate that highly strained [12]DBA **1a** was produced in an argon matrix at 20 K and it was characterized successfully by UV−vis and FT-IR spectra.

To investigate the C≡C stretching vibrations of triyne unit of **1a** in more detail, irradiation of the precursor **3a** and then Raman spectroscopic measurement was carried out in a neon matrix at 5 K. After irradiation of **3a**, photoproduct **1a** was observed by UV−vis and IR spectroscopy as was in an argon matrix. However, the Raman spectra of **1a**, even of **3a**, could not be recorded because of the disturbance by strong fluorescence from **3a**.

Kinetic Stability of Highly Strained DBAs 1a, 1b, and Their Homologues. To elucidate the feature of the deformed triyne units in **1a** and **1b**, we compared the geometries and kinetic stability of **1a** and **1b** with those of related DBAs with different number of carbon atoms and topologies of the annulene ring. The theoretical or experimental bond angles of the strained acetylene units and the characterization status of [8]DBAs **17**[36] and **18**,[37] [10]DBA **19**,[12] [12]DBAs **1a** and **20**,[38] and [14]DBA **1b** are listed in Table 1.

Structural optimization of **17** by the DFT calculation indicates that **17** does not possess a planar conformation but it has a C_2 symmetrical structure with an approximately 50° twist between the benzene rings, owing to the steric repulsion between the closely located aromatic hydrogen atoms. The diyne unit of **17** is extremely deformed from linearity; the bending angles are predicted to be 45° and 41°. Because of this extraordinary distortion, attempts to prepare **17** by elimination reactions from the corresponding bromide turned out unsuccessful.[36] On the other hand, its geometrical isomer **18**,[39] whose benzene rings are located on the opposite side of the eight-membered ring, is kinetically stable and is fully characterized, even though its X-ray crystal structure shows that the triple bond is highly deformed from linearity by 24°.[37b] Though [10]DBA **19** is only reported in connection with its theoretical NICS value,[12] it must be difficult to isolate it because of its significantly strained diyne moiety. Further ring enlargement to [12]-DBA **1a** makes the situation worse; the bent angle of the central triple bond of **1a** is more than 30°. Thus, as described above, **1a** was only characterized in matrices

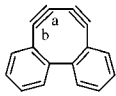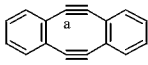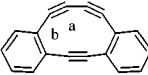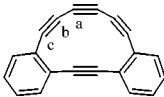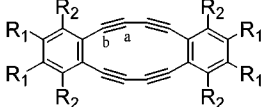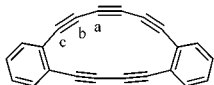(36) Wong, H. N. C.; Sondheimer, F. *J. Org. Chem.* **1980**, *45*, 2438−2440.

(37) (a) Wong, H. N. C.; Garratt, P. J.; Sondheimer, F. *J. Am. Chem. Soc.* **1974**, *96*, 5604−5605. (b) Destro, R.; Pilati, T.; Simonetta, M. *J. Am. Chem. Soc.* **1975**, *97*, 658−659.

(38) (a) Behr, O. M.; Eglinton, G.; Galbraith, A. R.; Raphael, R. A. *J. Chem. Soc.* **1960**, 3614−3625. (b) Zhou, Q.; Carroll, P. J.; Swager, T. M. *J. Org. Chem.* **1994**, *59*, 1294−1301. (c) Tovar, J. D.; Jux, N.; Jarrosson, T.; Khan, S. I.; Rubin, Y. *J. Org. Chem.* **1997**, *62*, 3432−3433. (d) Tovar, J. D.; Jux, N.; Jarrosson, T.; Khan, S. I.; Rubin, Y. *J. Org. Chem.* **1998**, *63*, 4856. (e) Bunz, U. H. F.; Enkelmann, V. *Chem. Eur. J.* **1999**, *5*, 263−266. (f) Gallagher, M. E.; Anthony, J. E. *Tetrahedron Lett.* **2001**, *42*, 7533−7536. (g) Nishinaga, T.; Nodera, N.; Miyata, Y.; Komatsu, K. *J. Org. Chem.* **2002**, *76*, 6091−6096.

(39) (a) Vogler, H. *Tetrahedron* **1979**, *35*, 657−661. (b) Vogler, H. *J. Am. Chem. Soc.* **1978**, *100*, 7464−7471. (c) Stollenwerk, A. H.; Kannellakopulos, B.; Vogler, H. *Tetrahedron* **1983**, *39*, 3127−3129. (d) Wilcox, C. F., Jr.; Weber, K. A. *J. Org. Chem.* **1986**, *51*, 1088−1094.

TABLE 1. Theoretical or Experimental Bond Angles and Characterization Status of DBAs 1a, 1b, and 17−20

compound		angles / deg.	characterization status	ref.
	17	a. 135.1[a,b] b. 139.0	unknown	36
	18	a. 155.8[c]	spectroscopic characterization and X-ray analysis	37
	19	a. 154.5[a,d] b. 153.4	unknown	12
	1a	a. 149.0[a,d] b. 156.9 c. 164.0	UV-vis and IR spectra in an Ar matrix at 20 K	this work
	20	a. 167.1[e] b. 165.4	spectroscopic characterization and X-ray analysis	38
	1b	a. 161.0[a,d] b. 167.2 c. 161.9	^{1}H and ^{13}C NMR spectra in solution at 303 and 243 K	this work

[a] The angles are theoretical values calculated by the DFT method at the B3LYP/6-31G* level. [b] The molecule has a C_2-symmetrical structure with an approximately 50° twist between the benzene rings. [c] The angles are determined by X-ray crystallographic analysis. [d] The molecule has C_{2v} symmetrical structure. [e] Listed angles are for **20** (R[1] = *n*-Bu, R[2] = H) from ref 38b.

at low temperatures. In contrast with **1a**, the symmetrical isomer **20**[38] and a number of its derivatives are successfully synthesized and are found to be stable at ambient temperature. The remarkable difference between the stabilities of **1a** and **20** is attributed to the presence of highly deformed triyne unit in **1a**. Finally, although [14]DBA **1b** having both diyne and triyne bridges was detected in solution, its isolation was not achieved because of its lability. These results indicate that the kinetic stabilities of DBAs are related to the symmetry of the annulene rings; the more symmetric the rings are, the more stable DBAs are, since the triple bond are increasingly deformed with decreasing symmetry.

Aromaticity of [14]DBA 1b and its Precursor 3b. As mentioned above, [12]DBA **1a** was too reactive for observation by ^{1}H NMR spectroscopy in solution. Therefore, it is not possible to discuss its tropicity on the basis of the experimental ^{1}H NMR chemical shifts. On the other hand, the ^{1}H NMR spectra of the less strained homologue **1b** was observed. As shown in Figure 3b, the aromatic protons of **1b** show distinctly different chemical shifts from those of its precursor **3b** though both have a [14]annulene ring. These differences can be attributed to the following factors, (1) increase or decrease of diatropicity of **1b** because of the rehybridization of the $C(sp^2)-C(sp^2)$ bond into the $C(sp)-C(sp)$, (2) change of

local anisotropy due to the triple bond[39] because of the geometrical change, and (3) change of anisotropy due to the 14-membered macrocycle because of the geometrical change. To clarify which factors dominate the difference of the chemical shift between **1b** and **3b**, we carried out a theoretical study for **1b** and **3b**.

Theoretical chemical shifts of the aromatic protons and the NICS values at the center of the 14-membered rings were calculated by the GIAO-DFT method on the B3LYP/6-31G*-optimized geometries. The results are listed in Table 2. The theoretical chemical shifts of the aromatic protons of **1b** and **3b** show reasonable agreement with those observed experimentally. As indicated by the values $\Delta\delta_{(1b-3b)}$, H_a and H_d, which are located close to the 14-membered cycle, are predicted to show distinct upfield shift (H_a: −0.45 ppm) or downfield shift (H_d: +0.12 ppm), respectively, upon structural change from **3b** to **1b**. On the other hand, H_b and H_c are not predicted to show much change. The NICS values may indicate that **1b** (−5.70) is slightly more diatropic than **3b** (−4.32). However, since the distance between the center of the ring and the ring carbon of **1b** is different from that of **3b**,[40] anisotropy experienced at the center of 14-membered ring of **1b**

(40) The distance between the center of the ring and the adjacent sp carbons (C1 and C11) in **1b** are 2.19 and 1.82 Å, respectively, while the corresponding distance in **3b** are 2.80 and 2.07 Å, respectively.
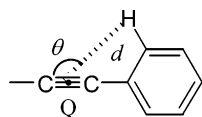
FIGURE 8. Schematic representation for geometrical parameters θ and d.

TABLE 2. Theoretical ^{1}H NMR Chemical Shift and NICS Values for 1b−d and 3b−d

	chemical shift[a]				
	H_a	H_b	H_c	H_d	NICS
1b	7.55	7.55	7.58	8.02	−5.7
	(7.59)	(7.59)	(7.59)	(7.92)	
3b	8.00	7.57	7.51	7.91	−4.4
	(7.83)	(7.54)	(7.50)	(7.76)	
$\Delta\delta_{(1b-3b)}$	−0.45	−0.02	+0.06	+0.12	
1c	7.15	7.07	7.08	7.35	
3c	7.32	7.08	7.08	7.22	
$\Delta\delta_{(1c-3c)}$	−0.17	−0.01	+0.00	+0.13	
1d	6.89	7.07	7.06	7.28	
3d	7.17	7.06	6.98	7.07	
$\Delta\delta_{(1d-3d)}$	−0.28	+0.01	+0.08	+0.21	

[a] Observed chemical shifts are given in parentheses.

TABLE 3. Geometrical Parameters for 1b and 3b

	H_a		H_d	
	d/Å	θ/deg	d/Å	θ/deg
1b	3.23	152.1	3.11	139.5
3b	3.08	137.7	3.16	144.4
$\Delta_{(1b-3b)}$	+0.15	+14.5	−0.05	−5.0

should be different from that of **3b** and, therefore, it is difficult to compare the tropicities of **1b** and **3b** on the basis of their NICS values.

To estimate the change of local anisotropy due to the triple bond induced by the geometrical change, we defined geometrical parameters d and θ as shown in Figure 8. The parameter d denotes the distance between the aromatic proton (H_a or H_d) and the center (Q) of the adjacent triple bond (C2≡C3 or C10≡C11), and θ refers to the angle H−Q−C. The value, Δd, is the difference between $d(\textbf{3b})$ and $d(\textbf{1b})$, and $\Delta\theta$ is the difference between $\theta(\textbf{3b})$ and $\theta(\textbf{1b})$. The values of d, Δd, θ, and $\Delta\theta$ for the optimized structures of **1b** and **3b** are shown in Table 3. The notable changes are the remarkably widened $\theta(H_a)$ by 14.5° and shortened $\theta(H_d)$ by 5.0°. Additionally, the distance $d(H_a)$ is considerably lengthened by 0.15 Å, while $d(H_d)$ is only slightly shortened by 0.05 Å. To estimate the effect on the local anisotropy of the triple bond, we calculated the theoretical chemical shifts for the hypothetical acyclic molecules **1c** and **3c** and the larger structures **1d** and **3d**, whose bond lengths and angles are kept same as those of **1b** and **3b**, respectively. Theoretical chemical shifts of **1c**, **3c**, **1d**, and **3d**, and $\Delta\delta_{(1c-3c)}$ (the difference the between chemical shifts of **3c** and those of **1c**) and $\Delta\delta_{(1d-3d)}$ (the difference between the chemical shifts of **3d** and those **3d**) are shown in Table 2. It turned out that the geometrical change of **3c** into **1c** would make H_a shift upfield (−0.17 ppm), while it would shift H_d downfield (+0.13 ppm). Accordingly, for H_a, more than one-thirds (−0.17 ppm) of the observed upfield shift (−0.45 ppm) is ascribed to the change of local anisotropy. The residual upfield shift may be ascribed

to the decrease of diatropicity of the 14-membered ring and/or the decrease of anisotropic effect due to increasing distance. For H_d, most of the observed downfield shift (+0.12 ppm) can be attributed to the local anisotropy effect (+0.13 ppm). The more extended structures **1d** and **3d** are expected to reproduce better the chemical shifts due to the local anisotropic effect for **1b** and **3b**. As in the case of **1c** and **3c**, the geometrical change of **3d** into **1d** would make H_a shift upfield (−0.28 ppm), while it would shift H_d downfield (+0.21 ppm). Accordingly, even after subtracting the contribution of the local anisotropic effect, H_a and H_b of **1b** would show another upfield by 0.17 and 0.09 ppm, respectively. Since both H_a and H_d are thus expected to show upfield shift, it is deduced that the diatropicity of the 14-membered annulene ring of **1b** is slightly smaller than that of **3b**. This may be due to the smaller conjugation energy between the adjacent triple bonds, i.e., 1,3-butadiyne than that of double bonds,[41] though there exists controversy regarding this issue.[42]

1c (geometry fixed as that of **1b**)
3c (geometry fixed as that of **3b**)

1d (geometry fixed as that of **1b**) **3d** (geometry fixed as that of **3b**)
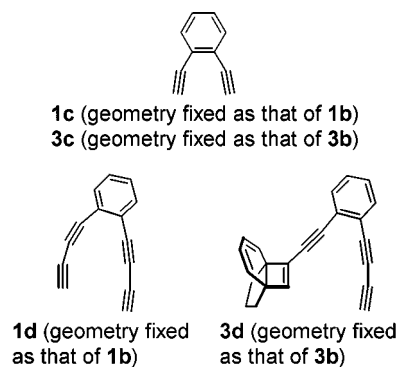
Conclusion

We prepared [4.3.2]propellatriene-annelated DBAs **3a** and **3b** as precursors of dibenzotetrakisdehydro[12]- and dibenzopentakisdehydro[14]annulenes **1a** and **1b** having a highly distorted triyne unit, and generated **1a** and **1b** by their photochemical [2 + 2] cycloreversion. Irradiation of [12]DBA **3a** in a furan or THF solution gave [4 + 2] adducts **13a** and **14a**, respectively. Though **1a** was too reactive for observation by ^{1}H NMR spectroscopy, it was successfully characterized by UV−vis spectra in a MTHF matrix at 77 K and by FT-IR spectra in an argon matrix at 20 K. On the other hand, [14]DBA **1b** was characterized by ^{1}H and ^{13}C NMR spectra in THF-d_8 solutions at ambient temperatures as well as by UV−vis spectrum in a MTHF matrix at 77 K. Upon structural change of **3b** into **1b**, chemical shifts of aromatic protons moved substantially, which is attributed to the decrease of tropicity of the 14-membered in addition to the change of the local acetylenic anisotropy.

Experimental Section

Synthesis of Precursor 3a (Method A). A suspension of **5**[21c,e] (407 mg, 1.32 mmol) and powdered KOH (670 mg, 11.9 mmol) in benzene (20 mL) was deoxygenated several times by freeze and thaw cycles (10^{-1} Torr). The mixture was stirred

(41) Rogers, D. W.; Matsunaga, N.; Zavitsas, A. A.; McLafferty, F. J.; Liebman, J. F. *Org. Lett.* **2003**, *5*, 2373−2375.
(42) Kollmar, H. *J. Am. Chem. Soc.* **1979**, *101*, 4832−4840.

at 80 °C with continuous removal of the solvent containing acetone. After 30 min, water and 10% HCl were added to the reaction mixture and it was extracted with ether. The extract was washed with brine. The organic layer was dried over anhydrous $MgSO_4$, filtered, and concentrated to a small volume. The residue was subject to column chromatography (silica gel, hexane) to afford a colorless solution of **4** in hexane. The solvent was replaced by a small amount of Et_3N by evaporation followed by immediate dilution, and the solution was used in next reaction immediately.

The deoxygenated solution of **4**[21c,e] and **6**[26] (347 mg, 806 μmol) in Et_3N (100 mL) was added dropwise to a deoxygenated suspension of $Pd(PPh_3)_4$ (194 mg, 168 μmol) and CuI (63 mg, 330 μmol) in Et_3N (10 mL) over 12 h with stirring at 60 °C. After stirring for another 9 h at 60 °C, the solvent was removed in vacuo and the reaction mixture was diluted with ether and 10% HCl. The mixture was extracted with ether, and the extract was washed with saturated $NaHCO_3$ solution and brine. The organic layer was dried over anhydrous $MgSO_4$, filtered, and concentrated to give 187 mg of a dark viscous oil. The product was purified by column chromatography (silica gel, 1% AcOEt in hexane) followed by preparative HPLC to afford 4.2 mg (1%) of **3a** as a yellow solid along with 6.5 mg (2%) of **7** and 18.2 mg (6%) of **8**. **3a**: mp > 184 °C dec; ^{1}H NMR (270 MHz, CDCl$_3$, 30 °C) δ 7.13−6.94 (m, 8H), 5.92−5.87 (m, 2H), 5.81−5.77 (m, 2H), 1.94 (dd, J = 12.7, 5.8 Hz, 2H), 1.78−1.59 (m, 2H), 1.24−1.13 (m, 2H); ^{13}C NMR (67.8 MHz, CDCl$_3$, 30 °C) δ 137.4 (q), 132.9 (t), 130.7 (t), 128.7 (t), 128.5 (t), 128.2 (q), 127.7 (t), 126.2 (q), 121.8 (t), 97.5 (q), 92.7 (q), 88.0 (q), 55.6 (q), 33.1 (s), 19.1 (s); IR (KBr) 3057, 3029, 2952, 2847, 2181, 1638, 1484, 749 cm^{-1}; UV (CHCl$_3$, 30 °C) λ_{max} (log ϵ) 273 (4.8), 283 (4.7), 291 (4.7), 302 (5.0), 338 (3.5), 349 (3.5), 364 (3.6), 391 (3.1), 411 (3.2), 423 (3.2), 441 (3.1), 449 (3.1), 463 (3.0), 496 (2.6) nm; MS (LD-TOF) m/z 366.2 (M$^-$), 248.1 (M$^-$ − 118.1). Anal. Calcd for C$_{29}$H$_{18}$: C, 95.05; H, 4.95. Found: C, 94.68; H, 4.85. **7**: ^{1}H NMR (270 MHz, CDCl$_3$, 30 °C) δ 7.78 (dd, J = 7.7, 1.2 Hz, 2H), 7.60−7.57 (m, 4H), 7.43−7.40 (m, 2H), 7.28 (ddd, J = 7.4, 7.4, 1.7 Hz, 2H), 7.24 (ddd, J = 7.4, 7.4, 1.7 Hz, 2H), 7.10 (ddd, J = 7.7, 7.7, 1.2 Hz, 2H), 6.88 (ddd, J = 7.7, 7.7, 1.7, 2H), 5.88−5.81 (m, 4H), 2.09−2.04 (m, 2H), 1.30−1.18 (m, 4H); MS (APCI) m/z 796.5 (M$^-$) 677.7 (M$^-$ − 118.8). **8**: ^{1}H NMR (270 MHz, CDCl$_3$, 30 °C) δ 7.82−7.79 (m, 2H), 7.65−7.61 (m, 2H), 7.58 (dd, J = 7.7, 1.7 Hz, 2H), 7.51−7.47 (m, 2H), 7.38−7.29 (m, 6H), 6.97 (ddd, J = 7.7, 7.7, 1.5 Hz, 2H), 5.90−5.80 (m, 8H), 2.09−1.95 (m, 4H), 1.31−1.20 (m, 8H); MS (APCI) 986.2 (M$^-$), 868.2 (M$^-$ − 118.0), 750.2 (M$^-$ − 236.0).

Method B. To a deoxygenated suspension of **5** (648 mg, 2.10 mmol), **6** (902 mg, 2.10 mmol), CuI (21 mg, 0.11 mmol), Pd-(PPh$_3$)$_4$ (257 mg, 0.23 mmol), PPh$_3$ (55 mg, 0.21 mmol), and tricaprylmethylammonium chloride (270 mg, 0.63 mmol) in benzene (200 mL) was added 2.5 N solution of NaOH (20 mL), and the reaction mixture was stirred at 80 °C under argon. After 8 h, another 2.5 N NaOH solution (20 mL) was added and the reaction was continued for another 7 h. After the mixture was cooled to room temperature, it was diluted with 10% HCl and extracted with AcOEt. The extract was washed with saturated NaHCO$_3$ solution, water, and brine. The organic layer was dried over anhydrous MgSO$_4$, filtered, and concentrated to give a dark viscous oil. The product was purified by column chromatography (silica gel, 10% AcOEt in hexane) followed by preparative HPLC to afford 376 mg (49%) of **3a** as a yellow solid.

Synthesis of Acyclic Tetrayne Derivative 12. A solution of **11**[28] (938 mg, 3.32 mmol) dissolved in piperidine/THF (10 mL, 5:1 v/v) was added dropwise over 45 min to a deoxygenated suspension of dichloropropellatriene **10**[21c,e] (266 mg, 1.25 mmol), Pd$_2$(dba)$_3$·CHCl$_3$ (52 mg, 0.050 mmol), CuI (65 mg, 0.34 mmol), and PPh$_3$ (112 mg, 0.425 mmol) in piperidine/THF (2 mL, 5:1 v/v) with stirring at 60 °C. After stirring for 8 h at 60 °C, the reaction mixture was filtered through a short column of silica gel and the solvent was removed in vacuo to give a

dark viscous oil. The products were purified by column chromatography (silica gel, 1% AcOEt in hexane) followed by preparative HPLC to afford 362 mg (41%) of **12** as an orange viscous oil, together with 233 mg (46%) of monosubstitution product as a pale yellow oil. **12**: ^{1}H NMR (270 MHz, 30 °C, CDCl$_3$) δ 7.49−7.43 (m, 4H), 7.24−7.19 (m, 4H), 5.93−5.84 (m, 4H), 2.10−2.04 (m, 2H), 1.63−1.55 (m, 2H), 1.32−1.17 (m, 2H), 1.11 (s, 42H); ^{13}C NMR (67.8 MHz, 30 °C, CDCl$_3$) δ 132.9 (t), 132.8 (t), 132.4 (q), 128.8 (t), 127.9 (t), 127.7 (t), 125.6 (q), 125.3 (q), 121.6 (t), 105.2 (q), 95.4 (q), 93.5 (q), 85.6 (q), 56.3 (q), 33.2 (s), 18.9 (t), 11.5 (t); IR (KBr) 3060, 3027, 2942, 2864, 2361, 2343, 2156, 1473, 755 cm^{-1}; MS (EI) m/z 704.3 (M$^+$); HRMS calcd for C$_{49}$H$_{60}$Si$_2$ 704.423, found 704.421. **Monosubstitution product**: ^{1}H NMR (270 MHz, 30 °C, CDCl$_3$) δ 7.49−7.43 (m, 2H), 7.22−7.14 (m, 2H), 5.96−5.79 (m, 4H), 2.08−1.98 (m, 2H), 1.65−1.42 (m, 2H), 1.30−1.18 (m, 2H), 1.14 (s, 21H); ^{13}C NMR (67.8 MHz, 30 °C, CDCl$_3$) δ 132.9, 132.7, 130.6, 128.9, 128.1, 127.8, 127.4, 125.9, 125.7, 124.9, 122.4, 121.5, 105.0, 95.5, 92.7, 82.4, 59.5, 56.2, 32.4, 31.8, 18.9, 18.8, 11.5; IR (KBr) 3057, 3029, 2943, 2865, 2359, 2157, 755 cm^{-1}; MS (EI) m/z 458.2 (M$^+$); HRMS calcd for C$_{30}$H$_{35}$Cl 458.220, found 458.218.

Synthesis of Precursor 3b. A 1.0 M solution of Bu$_4$NF in THF (3.27 mL) and AcOH (294 mg, 4.90 mmol) were added dropwise to a solution of **12** (329 mg, 0.467 mmol) in THF (20 mL) with stirring at room temperature. After 4 h, the mixture was diluted with ether (20 mL) and washed with water and brine. The organic layer was dried over anhydrous MgSO$_4$ and filtered. After concentration, the product **9** was dissolved in a small volume of pyridine and was used immediately in the next reaction.

A solution of the terminal acetylene **9** dissolved in pyridine (300 mL) was added dropwise over 23 h to a solution of Cu-(OAc)$_2$ (8.36 g, 46.0 mmol) in pyridine (200 mL) with stirring at room temperature. After another 18 h, the reaction mixture was concentrated and filtered through a short column of silica gel (chloroform). Purification by preparative HPLC gave 138 mg (75%, for two steps) of **3b** as a pale yellow solid. **3b**: mp > 160 °C dec; ^{1}H NMR (270 MHz, 30 °C, CDCl$_3$) δ 7.90−7.82 (m, 2H), 7.80−7.72 (m, 2H), 7.52 (ddd, J = 7.4, 7.4, 1.7 Hz, 2H), 7.47 (ddd, J = 7.4, 7.4, 1.5 Hz, 2H), 6.12−5.91 (m, 4H), 2.27−2.16 (m, 2H), 1.70−1.39 (m, 4H); ^{13}C NMR (67.8 MHz, 30 °C, CDCl$_3$) δ 132.3 (q), 131.6 (t), 129,9 (t), 129.1 (t), 128.3 (t), 127.9 (t), 127.7 (q), 124.0 (q), 121.8 (t), 94.2 (q), 87.4 (q), 84.0 (q), 79.9 (q), 56.7 (q), 33.7 (s), 19.0 (s); IR (KBr) 3057, 3030, 2952, 2928, 2844, 2204, 2147, 1597, 1470, 747 cm^{-1}; UV (30 °C, CDCl$_3$) λ_{max} (log ϵ) 415 (3.0), 384 (4.3), 355 (4.3), 343 (4.3), 321 (5.1), 310 (4.7), 301 (4.8), 263 (4.4) nm; MS (FAB) m/z 390.1 (M$^+$). Anal. Calcd for C$_{31}$H$_{18}$: C, 95.35; H, 4.65. Found: C, 95.14; H, 4.60.

Photolysis of 3a in THF-d_8. A solution of **3a** (6.0 mg, 16 μmol) dissolved in THF-d_8 (750 μL) was placed in a quartz NMR tube. The solution was deoxygenated by bubbling argon for 5 min before irradiation with a low-pressure mercury lamp (60 W) at room temperature for 31 h. The progress of the photolysis was monitored by ^{1}H NMR spectroscopy. The color of the solution of **3a** turned dark and a film was formed on the wall of the tube after irradiation.

Isolation of [4 + 2] Adduct 13a. A solution of **3a** (45 mg, 0.12 mmol) dissolved in THF (30 mL) was placed in a quartz tube and deoxygenated by bubbling argon. The solution was irradiated with a low-pressure mercury lamp (60 W) for 30 h in a water bath. The color of the solution of **3a** turned brown. After removal of the solvent in vacuo, the product was purified by column chromatography (silica gel, 5% AcOEt in hexane to chloroform) followed by preparative HPLC to afford 6.8 mg (18%) of **13a** as a yellow solid together with recovered **3a** in 44% yield. **13a**: mp > 150 °C dec; ^{1}H NMR (400 MHz, CD$_2$Cl$_2$, 30 °C) δ 7.08−6.88 (m, 16H), 6.37−6.33 (m, 2H), 3.31−3.29 (m, 2H), 2.09−2.03 (m, 2H), 1.56−1.49 (m, 4H); ^{13}C NMR (100 MHz, CD$_2$Cl$_2$, 30 °C) δ 138.9, 137.7, 133.4, 132.7, 132.5, 131.8, 131.2, 129. 5, 129.2, 128.5, 127.6, 127.4, 126.5, 100.5, 99.4, 94.1, 93.22, 93.18, 88.2, 64.2, 47.7, 30.1, 27.6; IR (KBr)

3057, 2954, 2922, 2857, 2210, 2177, 1486, 1470, 759, 747 cm^{-1}; MS (FAB) *m/z* 614.3 (M$^+$).

Isolation of [4 + 2] Furan Adduct 14a. A solution of **3a** (31 mg, 84 μmol) dissolved in fruan (50 mL) was placed in a quartz tube. The solution was deoxygenated by argon bubbling before irradiation with a low-pressure mercury lamp for 32 h in an ice−water bath. The furan was removed in vacuo and the product was isolated by column chromatography (silica gel, 1% AcOEt in hexane) followed by preparative HPLC to afford 5.7 mg (20%) of **14a** as an orange solid together with recovered **3a** in 50% yield. **14a**: mp > 160 °C dec; ^{1}H NMR (270 MHz, CDCl$_3$, 30 °C) δ 7.09−6.93 (m, 10H), 5.27 (dd, J = 1.0, 1.0 Hz, 2H); ^{13}C NMR (67.8 MHz, CDCl$_3$, 30 °C) δ 146.5 (q), 142.1 (t), 132.7 (t), 130.8 (t), 129.1 (t), 128.8 (t), 127.8 (q), 126.6 (q), 108.0 (q), 93.0 (q), 88.9 (q), 84.5 (q); IR (KBr) 3053, 3028, 2195, 2174, 1485, 874, 854, 751 cm^{-1}; UV (CHCl$_3$, 30 °C) λ $_{max}$ (log ϵ) 262 (4.7), 276 (4.8), 307 (sh, 4.5), 318 (4.7), 345 (3.3), 359 (3.3), 376 (3.4), 436 (sh, 3.1), 470 (3.1), 490 (sh, 3.0), 525 (2.7) nm; MS (LD-TOF) *m/z* 316.1 (M$^-$).

Photolysis of 3b in THF-d_8. A solution of **3b** (3.2 mg, 8.2 μmol) dissolved in THF-d_8 (750 μL) was placed in a quartz NMR tube. The solution was deoxygenated several times by freeze and thaw (10^{-3}−10^{-4} Torr) cycles and then sealed. The solution was irradiated for 24 h with a low-pressure mercury lamp in an EtOH bath cooled at 220 K equipped with a refrigerating device. The color of the solution turned dark and dark precipitates were formed in the tube after irradiation. Standing the solution for 56 h at 30 °C led to the decomposition of **1b** and the formation of **13b** (see Figure 5b). **1b**: ^{1}H NMR (400 MHz, 30 °C, THF-d_8) δ 7.93−7.91 (m, 2H), 7.63−7.57 (m, 6H); ^{13}C NMR (400 MHz, −30 °C, THF-d_8) δ 132.3, 129.6, 129.23, 129.17, 127.5, 125.1, 101.5, 82.0, 81.6, 80.4, 79.2.

Photolysis of 3b in Furan. A solution of **3b** (41.5 mg, 0.106 mmol) dissolved in furan (45 mL) was placed in a quartz tube. The solution was deoxygenated by argon bubbling and sealed. The solution was irradiated with a low-pressure mercury lamp (60 W) in a water bath for 26 h. The color of the solution turned dark and dark precipitates were formed in the tube after irradiation. The furan was removed in vacuo and the product was isolated by column chromatography (silica gel, 10% AcOEt in hexane) followed by preparative HPLC to afford a small amount of **14b** as a brown solid. The recovered starting material **3b** (32.8 mg) was irradiated again by same way for 20 h to afford 1 mg (2%) of **14b**. **14b**: ^{1}H NMR (400 MHz, CDCl$_3$, 30 °C) δ 7.96−7.94 (m, 2H), 7.83−7.81 (m, 2H), 7.59 (ddd, J = 7.6, 7.6, 1.5 Hz, 2H), 7.54 (ddd, J = 7.6, 7.6, 1.5 Hz, 2H), 7.30 (dd, J = 1.0, 1.0 Hz, 2H), 5.88 (dd, J = 1.0, 1.0 Hz, 2H); MS (APCI) *m/z* 341.2 (M$^+$ + 1).

Photolysis of 3a in a 2-Methyltetrahydrofuran (MTHF) Matrix. A solution of **3a** in MTHF (5.8×10^{-5} M) placed in a UV cell was degassed by freeze and thaw cycles (10^{-3}−10^{-4} Torr) and then sealed. The cell was immersed into a liquid

nitrogen vessel and the glass matrix was irradiated with a low-pressure mercury lamp (60 W) through a window of the vessel for 14 h. Photolysis was monitored by UV−vis spectroscopy (Figure 5). After irradiation, the matrix was thawed by warming to room temperature and then refrozen at 77 K to measure a UV−vis spectrum again (Figure 5, inset).

Photolysis of 3b in a MTHF Matrix. Photolysis of **3b** was carried out for 12 h with a matrix of **3b** in MTHF (6.2×10^{-6} M) according to the same procedure as that of **3a**. After irradiation, the matrix was thawed by warming to 303 K and left for 50 h at this temperature. The changes were monitored by UV−vis spectroscopy (Figure 6).

Photolysis of 3a in an Argon Matrix. Compound **3a** was vaporized at 150−155 °C and co-deposited with argon (99.9999%) on a CsI plate cooled at 20 K in a sample chamber whose pressure was kept at <10^{-3} Torr. Matrix-isolated precursor **3a** was photolyzed by using a forth harmonic generation (FHG) pulses of Nd:YAG laser (λ = 266 nm, 10 Hz, ca. 0.8 mJ cm^{-2} pulse^{-1}). Deposition-irradiation cycle was repeated seven times to increase the concentration of the photoproducts. In the cycle, the precursor **3a** was deposited for 15−20 min and then photolyzed by irradiation for 1−2 h. Both sides of the CsI substrate were used for the matrix preparation to avoid the peeling off the matrix: first to forth deposition was carried out on the one side, and fifth to seventh was on the other side. Total irradiation time was 12 h. The photolysis was followed by UV−vis (see Figure S5 in the Supporting Information) and FT-IR spectra.

Computational Methods. The DFT calculations were performed with the Gaussian 03 program package.[43] The geometries of the compounds were optimized by using the B3LYP method in combination with the 6-31G* basis set. The nature of the stationary points was assessed by means of vibration frequency analysis. The theoretical IR spectra of **1a**, **3a**, and indan were calculated for their optimized geometries. The chemical shifts and the NICS values of **1b** and **3b** were calculated by the GIAO-DFT method, where C_{2v} symmetry was adopted for the optimized structure of **1b**. Hypothetical molecules **1c**, **3c**, **1d**, and **3d** were constructed on the Gauss-View 03 by removal of the redundant part from the parent molecules **1b** and **3b** followed by attaching hydrogen atoms on the terminal carbon atoms with keeping the original bond angles (for **1d** and **3d**) or keeping the C≡C−H angles 180° (for **1c** and **3c**). The C−H bond lengths were kept 1.06622 Å for a C(sp)−H bond and 1.0833 Å for a C(sp^2)−H bond.

X-ray Crystallographic Structure Analyses. See the Supporting Information.

Supporting Information Available: Full-scale ^{1}H NMR spectra of **3a** and **3b** and their change upon photolysis, a full-scale ^{13}C NMR spectrum of **3b** after irradiation, UV−vis and full-scale FT-IR spectra of **3a** upon photolysis, optimized geometries of **1a**, **3a**, indan, **1b**, **3b**, **15a**, **17**, and **19** by the DFT calculations, theoretical IR spectra of **1a**, **3a**, and indan, theoretical chemical shifts of **1b**, **3b**, and **15a**, coordinates and theoretical chemical shifts of hypothetical molecules **1c**, **3c**, **1d**, **3d**, and **15b**, calculated Mulliken atomic charges of **15a** and **15b**, ^{1}H and ^{13}C NMR spectra of **3a**, **12**, **3b**, **13a**, and **14a**, X-ray crystal structures of **3a**, **3b**, **13a**, and **14a**, and X-ray crystallographic files of **3a**, **3b**, **13**, and **14** (CIF). This material is available free of charge via the Internet at http://pubs.acs.org.

JO047857P

(43) Frisch, M. J.; Trucks, G. W.; Schlegel, H. B.; Scuseria, G. E.; Robb, M. A.; Cheeseman, J. R.; Montgomery, J. A.; Vreven, T., Jr.; Kudin, K. N.; Burant, J. C.; Millam, J. M.; Iyengar, S. S.; Tomasi, J.; Barone, V.; Mennucci, B.; Cossi, M.; Scalmani, G.; Rega, N.; Petersson, G. A.; Nakatsuji, H.; Hada, M.; Ehara, M.; Toyota, K.; Fukuda, R.; Hasegawa, J.; Ishida, M.; Nakajima, T.; Honda, Y.; Kitao, O.; Nakai, H.; Klene, M.; Li, X.; Knox, J. E.; Hratchian, H. P.; Cross, J. B.; Adamo, C.; Jaramillo, J.; Gomperts, R.; Stratmann, R. E.; Yazyev, O.; Austin, A. J.; Cammi, R.; Pomelli, C.; Ochterski, J. W.; Ayala, P. Y.; Morokuma, K.; Voth, G. A.; Salvador, P.; Dannenberg, J. J.; Zakrzewski, V. G.; Dapprich, S.; Daniels, A. D.; Strain, M. C.; Farkas, O.; Malick, D. K.; Rabuck, A. D.; Raghavachari, K.; Foresman, J. B.; Ortiz, J. V.; Cui, Q.; Baboul, A. G.; Clifford, S.; Cioslowski, J.; Stefanov, B. B.; Liu, G.; Liashenko, A.; Piskorz, P.; Komaromi, I.; Martin, R. L.; Fox, D. J.; Keith, T.; Al-Laham, M. A.; Peng, C. Y.; Nanayakkara, A.; Challa-combe, M.; Gill, P. M. W.; Johnson, B.; Chen, W.; Wong, M. W.; Gonzalez, C.; Pople, J. A. *Gaussian 03*, revision B.03; Gaussian, Inc.: Pittsburgh, PA, 2003.